

Accurate measurement of diffusion rates of small molecules through polymers

P. Morrissey, D. Vesely*

Department of Materials Engineering, Brunel University, Uxbridge, Middlesex UB8 3PH, UK

Received 27 January 1999; accepted 5 May 1999

Abstract

The diffusion of methanol in PMMA and dodecane in PS has been studied by in situ dynamic observations using light microscopy. A specially constructed cell enabled accurate monitoring of the diffusion fronts as they advance into the polymer matrices. It is shown that the diffusion rate at the early stages of the process does not follow the rate predicted by square root from time behaviour and that swelling is also delayed. Analysis of the results indicated that the following equation gives an accurate correlation with the experimental data: $x = b(t^{1/2} - (1 - e^{-t^{1/2}}))$. It was also observed that voids can be filled up by the penetrant, representing diffusion against the concentration gradient and thus indicating that concentration driven mechanisms are not applicable to the systems studied in this work. © 1999 Elsevier Science Ltd. All rights reserved.

Keywords: Diffusion rate; Swelling; Light microscopy

1. Introduction

The diffusion of small molecules through polymers is one of their most important properties for all applications, especially for packaging materials, polymer coatings, drug delivery systems and ion selective membranes. It is important that a method is available to monitor these processes accurately. A comprehensive survey of the existing methods used to analyse the diffusion processes [1] concludes that light and electron microscopy, NMR Imaging and gravimetric analysis give the most accurate and reliable data. Unfortunately, most of the light microscopy methods reported in the literature label the penetrant, e.g. methanol stained with iodine [2–6], and in situ measurements which have much better accuracy than intermittent techniques are not available. NMR imaging is capable of measuring penetrant concentration profiles but has poor resolution (approximately 70 μm) [7,8], while gravimetric methods yield no information on the concentration profile of the penetrant and cannot take structural features into account. For this reason a special cell was developed which uses light microscopy to measure diffusion rates in situ, without the need to stain the penetrant. This was employed to monitor the rate of advancement of a diffusion front through a polymer, the

rate of swelling of the polymer and to investigate the effect of structural defects on the diffusion process.

The accurate measurements are needed in order to establish which diffusion mechanism is operational for a given matrix/penetrant system. In particular the concentration profile and the rate of diffusion must be measured independently. The measurements of mass uptake are therefore less valuable as they cannot differentiate between the concentration level and the penetration distance. The work presented here deals exclusively with the measurements of the diffusion rate. The diffusion front is sharp and provides good contrast in the light microscope. This offers an opportunity to carry out accurate in situ measurements of the progress of the diffusion front with time. The time dependence has been measured before but a final conclusion has not yet been reached. Some results indicate square root of time dependence for the penetrated distance (Fickian), others show direct time dependence (Case II sorption). A mixed dependence has also been reported and an attempt has been made to generalize the behaviour and assign a particular behaviour to a temperature range, controlled by the glass transition temperature.

2. Experimental technique

A special cell was developed for monitoring in situ the rate of advancement of the diffusion front into the polymer

* Corresponding author.

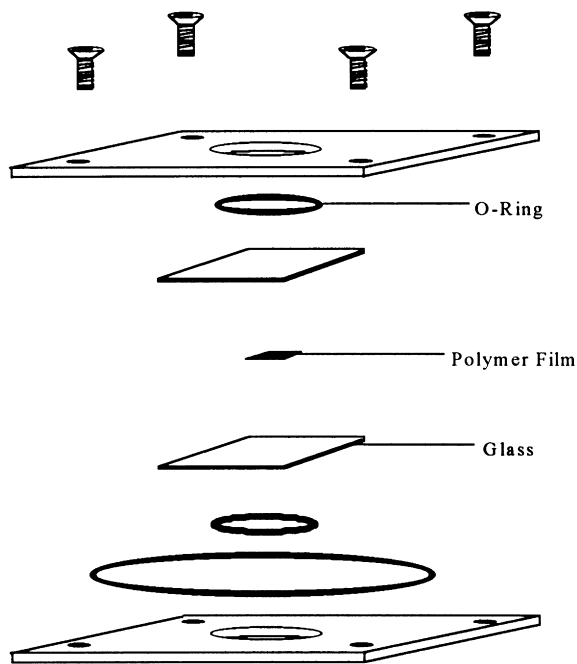


Fig. 1. Expanded view of the diffusion cell used for in situ measurements.

matrix (see Figs. 1 and 2). This was achieved by allowing the penetrant to come into contact with the edge of the polymer sample but not with the top or bottom surfaces. Swelling of the polymer by the penetrant helped in providing a perfect seal. The diffusion front can thus be viewed from above and its progress continuously and accurately monitored.

The cell was machined from two 3 mm thick plates of stainless steel. The polymer samples, which were in the form of a film approximately, $5 \text{ mm} \times 5 \text{ mm} \times 50 \mu\text{m}$, were placed between two square pieces of a glass slide $25 \text{ mm} \times 25 \text{ mm}$. This was then sandwiched between two Viton O-rings (19.95 mm in diameter and 2.58 mm thick) which fitted into the grooves on the two plates. A larger O-ring (45.75 mm in diameter and 3.53 mm thick) was used to provide a seal between the two steel plates clamped together by tightening screws. The thickness of the large O-ring and the depth of the grooves for the small O-rings were selected for the best seal. There were also two holes, 1 mm in

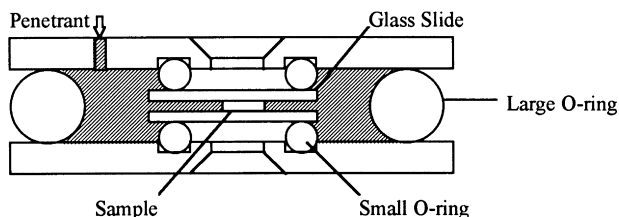


Fig. 2. Schematic diagram of the diffusion cell. The penetrant is contained in the shaded area sealed by the O-rings. The tightening screws outside the larger O-ring are not shown. The holes used for injection of the penetrant are sealed with a tape.

diameter, in the top plate which were used to inject and remove the penetrant from the cell.

The cell was placed on a temperature controlled hot stage which was mounted on a Leitz transmission light microscope with a 6.3 times long working distance objective lens. The temperature fluctuation of the sample mounted in the cell was measured with a thermocouple and was found to be $\pm 0.6^\circ$ at 70°C .

Diffusion processes were recorded by either mounting a camera on the microscope and taking micrographs at certain time intervals, or by using one of the two available CCD cameras. One of these was a black and white Kappa CCD with a 500×700 pixel resolution, while the other was a colour Wattec Wat-202 CCD with a resolution of 700×700 pixels. A Sony Hi-8 video recorder was used to record the diffusion processes. Oculus-TCX frame grabbing card was used to import the images from the video recorder onto a PC. PC-Image (version 3.1) software package was used to accurately measure the penetration distance of the diffusion front, using the line profiling option. It has the advantage over using the camera in that more images of the experiment can be recorded, but unfortunately it cannot record processes in excess of 3 h due to the limitations imposed by the video tapes.

3. Preparation of thin films

The PS film used in the diffusion cell was prepared by solvent casting. The PS had an average molecular weight of 280 000 and a density of 1.047 g/cm^3 (Aldrich). It was dissolved in 99.5% xylene (BDH) to 30% solids at room temperature and cast onto a clean glass slide and left for three days at room temperature before annealing at 70°C for 24 h and then under vacuum at 70°C for another 24 h. The concentration of the solvent in the film was monitored using a Nicolet 60 SX FTIR spectrometer. This was done using the xylene aromatic C–H out-of-plane bending vibration at 875 cm^{-1} , which was found to have zero intensity upon completion of the annealing process. The T_g was also measured before and after casting and was found to be 105°C for both samples.

The preparation of thin films of PMMA was the same as that used for PS. The polymer was dissolved to 30% solids in chloroform, cast into a film, left at room temperature for 24 h before annealing at 60°C for 24 h and then at 60°C under vacuum for another 24 h. The concentration of the chloroform in the film was monitored using its C–Cl stretching vibration at 757 cm^{-1} .

4. Results and discussion

4.1. Accuracy of data

In previous studies [2–6,9,10] the polymer samples were suspended in the penetrant and left there for time, t . On

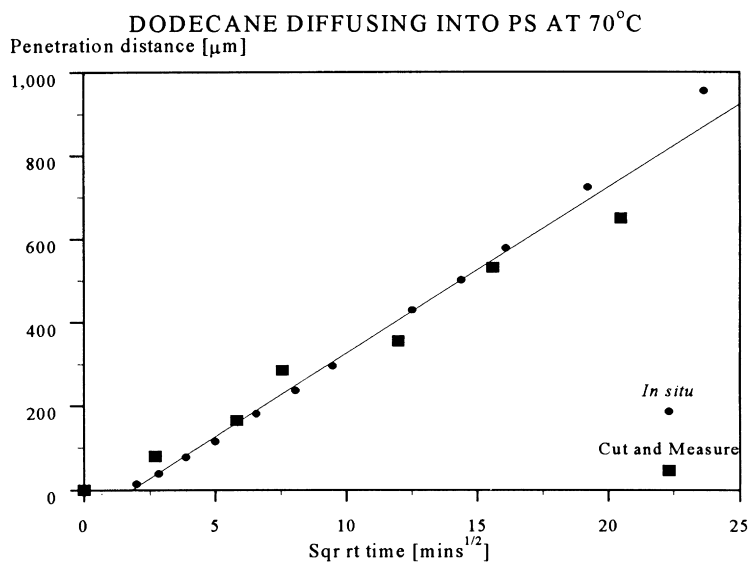


Fig. 3. Penetration distance dependence on square root of time for cut samples (squares) and for in situ measurements (dots) of dodecane in PS at 70°C. The in situ data are less scattered than the data from cut samples. The deviations from a straight line are due to changes in length (curvature) of the diffusion front.

cutting thin cross sections of the sample the penetrant diffusion layer was clearly visible under a light microscope, which made it possible to measure the penetration distance of the diffusion front. The rate of advancement of the diffusion front into the polymer matrix was then determined by repeating the above procedure for various diffusion times. This procedure was used to monitor the diffusion of dodecane into PS and the results are shown as the penetration distance versus time in Fig. 3. The graph clearly demonstrates that the rate of advancement is not linear with time but is linear with the square root of time. The inaccuracy of the data is mainly due to deformation of the thin sections (with 10–60 μm thickness) during the cutting procedure. This effect is compounded by the difference in hardness and rigidity between the outer swollen layer and the inner unswollen pure polymer region. Another source of inaccuracy is the fact that the test is a destructive one and thus a different sample had to be used for each diffusion time. These inaccuracies were, to some extent, eliminated by using the diffusion cell for in situ observation.

The micrographs of the progressing front in the diffusion cell are shown in Fig. 4(a) and (b). The stronger line is the edge of the polymer sample and the weaker line is the interface between the swollen and unswollen regions, i.e. the diffusion front, which moves into the polymer matrix with time. A calibrated graticule in the eyepiece of the microscope was used to measure the penetration distance of the diffusion front with time and the results given in the form of graphs of the rate of advancement of the diffusion front. In Fig. 3 the advancement of dodecane's diffusion front into PS with time at 70°C is presented for both methods. The data from the in situ measurements deviate from a straight line in the last two points as they were not corrected for the diminishing size of the diffusion front. Again it was found that the

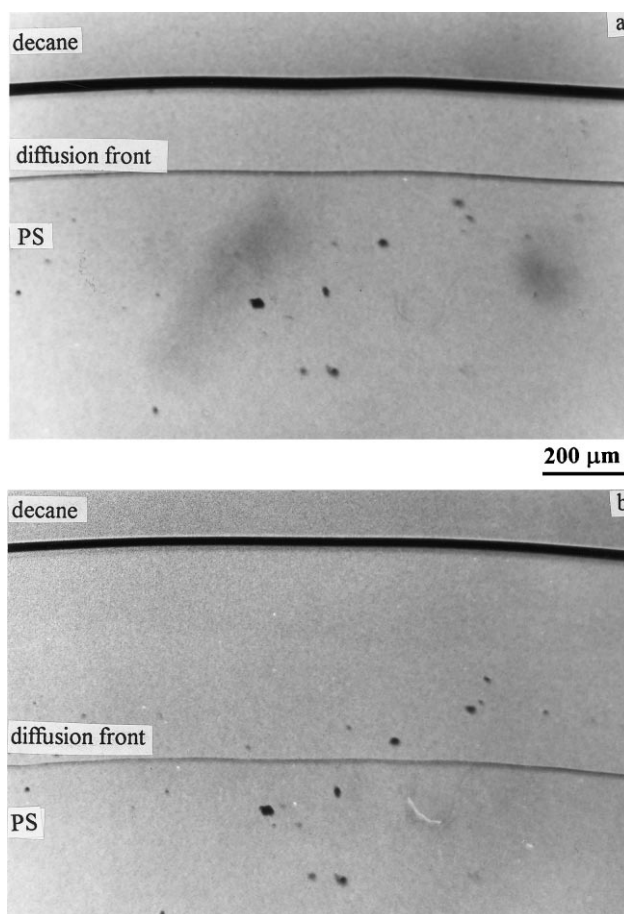


Fig. 4. (a) Light micrograph of the diffusion front of decane in PS at 70°C after 10 min, as seen in the diffusion cell. (b) Light micrograph of the diffusion front of decane in PS at 70°C after 60 min, same area as in (a).

LINE PROFILES OF PMMA/METHANOL DIFFUSION LAYERS

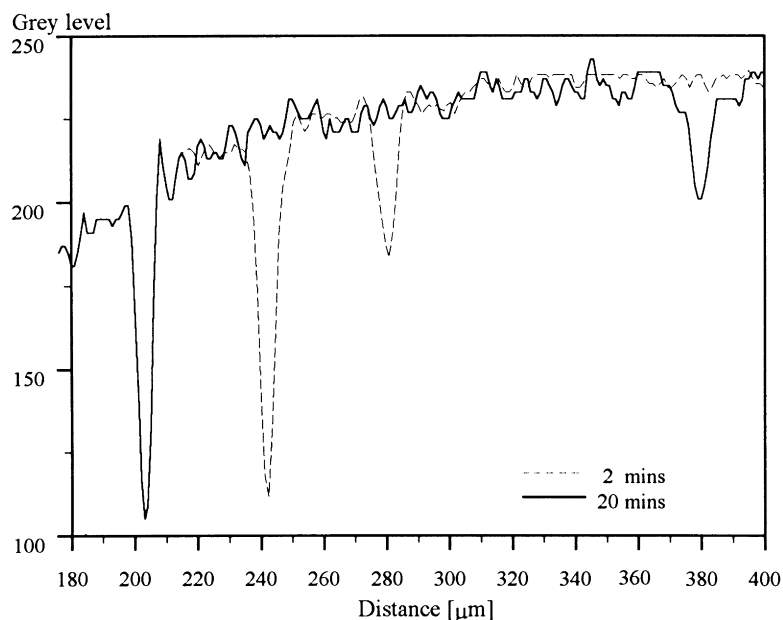


Fig. 5. Contrast line profile of video recorded diffusion of methanol in PMMA after 2 min (broken line) and 20 min (solid line). Larger peaks correspond to the penetrant/polymer interface, smaller peaks to the diffusion front.

rate of advancement of the diffusion front was linear with the square root of time, but the accuracy of the data had been improved to 0.9992. This compares favourably with the data from the cut and measure method which had a correlation coefficient of 0.9977, thus proving that using the diffusion cell increased the accuracy of the experiments. It also revealed an initial time lag which cannot be resolved with the data collected using the 'cut and measure' method, suggesting that it is either an artefact of the diffusion cell techniques or that it is a genuine part of the diffusion process

which did not show up in the cut and measure technique due to the high level of scatter of the data.

The accuracy of measuring the penetration distances was improved by using a video camera to record the diffusion processes and then using the line profiling option on 'PC-Image' software. This is demonstrated for two of the images of methanol diffusing into PMMA. Their respective line profiles are given in Fig. 5 and the accuracy of this measurement technique was found to be $\pm 2 \mu\text{m}$. The technique also has the advantage of recording 12 images a

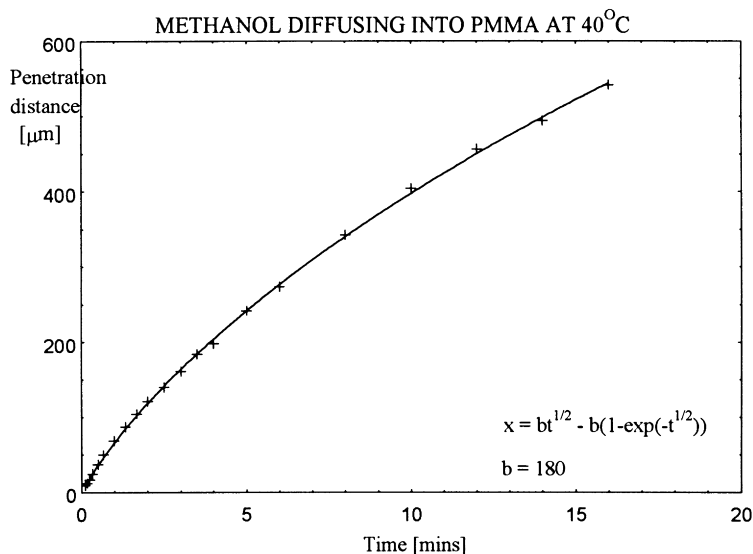


Fig. 6. Time dependence of the penetration distance for methanol in PMMA. The solid line is calculated using Eq. (1) for the best fit.

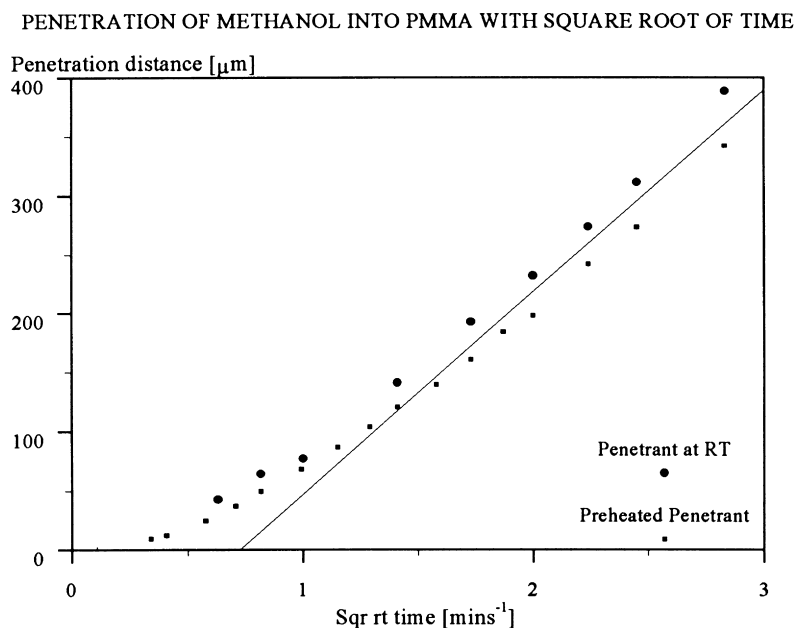


Fig. 7. Graph of penetration distance/square root of time for penetrant introduced at room temperature and at temperature of the cell at 40°C, showing that pre-heating has no effect on the initial slow diffusion rate (time lag).

second, thus enabling up to 12 measurements a second to be recorded. This allows for accurate measurements of the early stages of the diffusion processes that occur in seconds to those which occur over a number of days. Typical data are shown in Fig. 6 for methanol diffusing into PMMA at 40°C.

In the above experiment the penetrant was at room temperature when injected into a hot diffusion cell, therefore as it heats up in the cell, its rate of diffusion and hence the rate of advancement of the diffusion front will initially be slower. This could explain the time lag in reaching the square root from time behaviour. In order to investigate if this is the case the above experiment was repeated for methanol diffusing into PMMA, but this time the penetrant was preheated to the diffusion temperature before injecting it into the cell. The results are given in Fig. 7 and clearly show that preheating the penetrant has no effect on the initial time lag. The penetrant which was pre-heated has a slightly lower diffusion rate and not higher as expected. This small inaccuracy in the data is probably due to fluctuation of the temperature of the cell, or due to the differences in the sample. This result proves that the initial time lag is not due to the difference in temperature between the penetrant and polymer, but is a part of the diffusion process. Grinsted et al. [7] found the same result for MeOD diffusing into PMMA using NMR imaging. They described it as “an initial lag of anomalous diffusion” and suggested that it is caused by the plasticization of the polymer by the penetrant. After this initial lag the sample is sufficiently plasticized to accommodate the solvent almost immediately and thus the movement of the penetrant is no longer inhibited by the rate of polymer relaxation. Billovits and Durning [6] found a time lag for

methanol, acetone and dimethylformamide diffusing into PET using a gravimetric method and also showed that this effect increases with decreasing temperature.

4.2. Diffusion rate equation

There are good reasons to accept that the initial time lag is a valid part of the diffusion process. Statistical analysis of the penetration distance versus time data was carried out and it was found that they could be accurately fitted to Eq. (1), which is demonstrated on the data for the PMMA/methanol system in Fig. 6.

$$x = b(t^{1/2} - (1 - e^{-t^{1/2}})) \quad (1)$$

where x is the penetration distance, t the reduced time and b a constant. The PMMA/methanol experimental data can be directly compared to those in the literature, i.e. to Grinsted et al. [7] and Thomas and Windle [2–4]. As stated above, the data collected here and by Grinsted showed an initial time lag followed by square root from time advancement of the diffusion front. Thomas and Windle interpreted their data as a linear relationship between the rate of advancement of the diffusion front and time. However they used the ‘cut and measure’ technique to measure the penetration distance, which is not as accurate as the one described here. Also, close inspection of their data showed that the rate of advancement of the diffusion fronts slows down with time and that this effect increases with increasing temperature, thus indicating that their diffusion fronts do not strictly advance linearly with time.

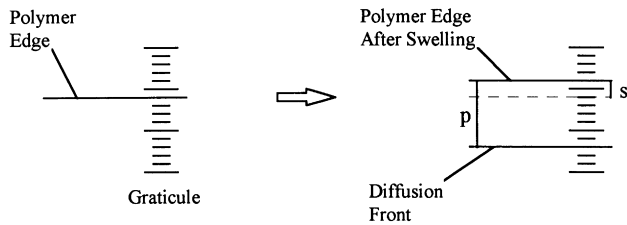


Fig. 8. Schematic diagram of the in situ measurement of the penetration distance and swelling, using a graticule.

4.3. Swelling rate

The diffusion cell also enabled the swelling of the polymer matrix during penetration of the diffusant to be measured in situ. This was done by measuring the movement of the edge of the sample with time using the graticule in the eyepiece (see Fig. 8). The distance travelled by the polymer edge, s , which is in the opposite direction to that of the penetrant diffusion, was taken to be the swelling distance and is given for the PMMA/methanol diffusion system in Fig. 9 along with the penetration distance with time data.

The results clearly show that both the diffusion and swelling processes slow down with time. On plotting the results against the square root of time (Fig. 10), both sets of data showed linear dependence.

4.4. Filling-up voids

An experiment was designed to understand the behaviour of a penetrant as it diffuses through a polymer sample containing voids. PS samples have been selected and cut

in such a way that they contain voids near the sample edge (Fig. 11(a)). The diffusion of hexane and decane into these samples was monitored using methods described earlier. It was observed that when the diffusion front reached the voids, a secondary diffusion front appeared at the contour of the void (voids B and C, Fig. 11(b)). The contour of the secondary front was weaker, indicating lower concentration. When the main diffusion front had passed the void, it disappeared without a trace (A in Fig. 11(b)), while a small proportion of voids B and C was still visible. At this stage voids B and C are still not completely filled up with the penetrant and the main diffusion front has not yet reached the tips of these voids.

From these observations it can be concluded that when the diffusion front reaches the void the penetrant vapour molecules mix with the trapped air in the void and quickly reach the entire surface of the void. They then enter into the polymer and the diffusion front propagates from the void contours. The contour of this diffusion front is lighter because of the thickness effect and also because the vapour swells the polymer less than the liquid.

The complete disappearance of the voids is more difficult to explain, as the penetrant has a slightly different refractive index to that of the swollen polymer and some contrast should therefore be present. It can be suggested that the swelling on its own will close the voids, however it is unlikely that voids of different sizes will be completely closed, even when the voids are flat and on the surface between the glass and the polymer, as the swelling of the polymer in the vicinity of the void would have to be greater than in the matrix. It is likely, that both mechanisms contribute to this effect. The penetrant is filling up the voids, the

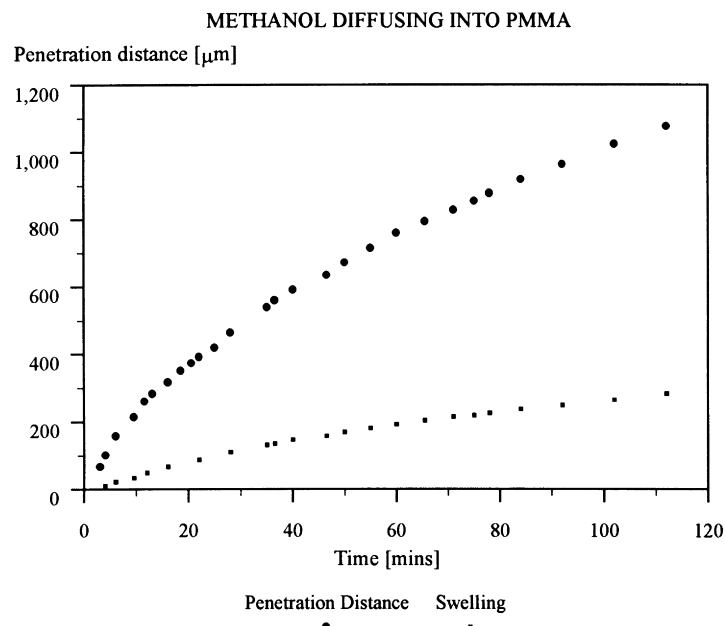


Fig. 9. Time dependence of penetration distance and swelling for methanol in PMMA at room temperature.

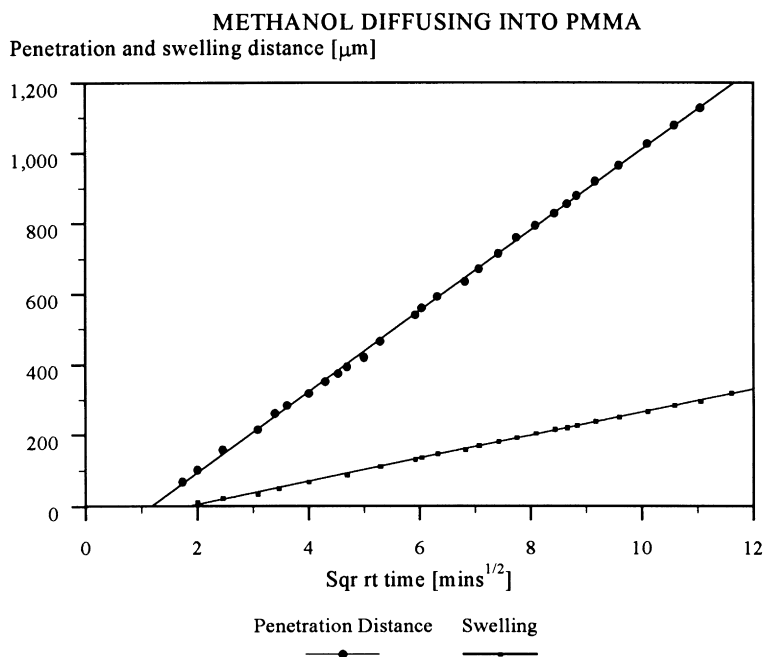


Fig. 10. Square root of time dependence of penetration distance and swelling for methanol in PMMA at room temperature, same data as in Fig. 9.

osmotic pressure will compress the remaining air in the voids forcing it to diffuse into the polymer, which is swollen and plasticized by the penetrant. The above mechanism is confirmed by NMR imaging [11] of acetic acid diffusion into epoxy with voids. In this case the voids are located in the middle of the samples, which can be confirmed and the voids filled up by the penetrant can be clearly distinguished from the matrix.

The consequences of the above observations are that the concentration gradient or the chemical potential are not the only driving forces for diffusion, and that partial vapour pressures and molecular interactions have also to be considered.

5. Conclusions

1. The accuracy of the penetration distance and swelling measurements has been substantially improved by using a cell for in situ observation with video recording and computer analysis.
2. The initial time lag at the start of the diffusion process has been verified, together with the advancement of the diffusion front with the square root of time.
3. The penetration distance with time data follows closely the relationship: $x = b(t^{1/2} - (1 - e^{-t^{1/2}}))$, where t is the time and x the penetration distance.
4. The penetrant diffuses into large voids present in the polymer matrix, fills them up and then diffuses further into the polymer ahead of the diffusion front. Presence of voids will therefore enhance the diffusion rate.

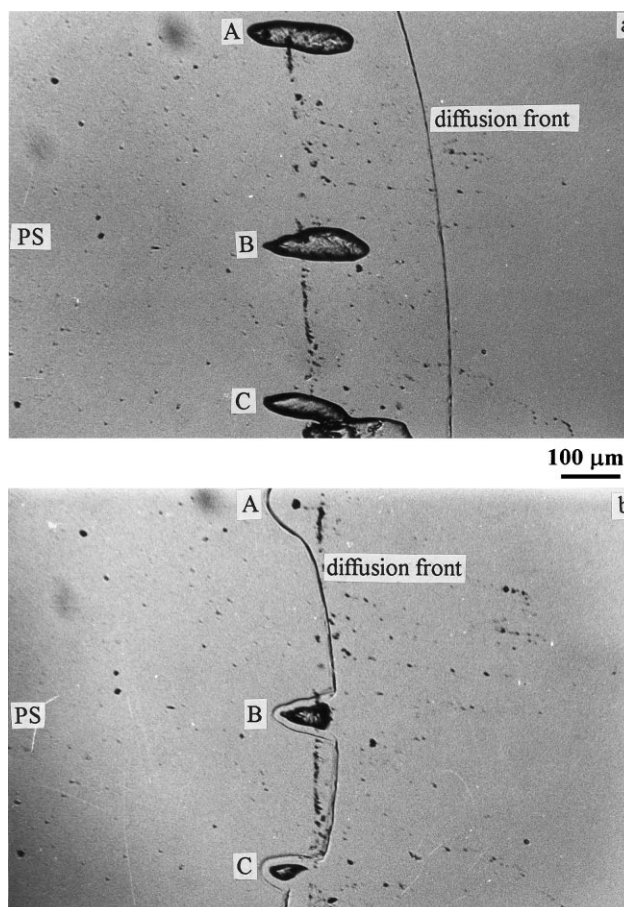


Fig. 11. (a) Light micrograph of hexane diffusion into PS at 40°C, large voids are visible. (b) Same area as in (a) at a later stage of diffusion. Voids filled up by the penetrant are visible, as well as the secondary diffusion front.

Acknowledgements

The financial support for a CASE award (P.M.) from EPSRC and Courtaulds Coatings (Holdings) Ltd. is gratefully acknowledged.

References

- [1] Morrissey P, Vesely D. To be published.
- [2] Thomas NL, Windle AH. *Polymer* 1978;19:255.
- [3] Thomas NL, Windle AH. *Polymer* 1980;21:613.
- [4] Thomas NL, Windle AH. *Polymer* 1981;22:627.
- [5] Kwei TK, Zupko HM. *Journal of Polymer Science: Part A-2* 1969;7:867.
- [6] Billovits GF, Durning CJ. *Polymer* 1988;29:1468.
- [7] Grinsted RA, Clark L, Koenig JL. *Macromolecules* 1992;25:1235.
- [8] Maffei P, Kiene L, Canet D. *Macromolecules* 1992;25:7114.
- [9] Parker MA, Vesely D. *Journal of Polymer Science B: Polymer Physics* 1986;24:1869.
- [10] Morrissey P, Vesely D. *Proceedings of Polymat'94*, 1994, p. 539
- [11] Dutheillet Y, Mantle M, Vesely D, Gladden L. To be published.